CHEMISTRY
A EUROPEAN JOURNAL

Supporting Information

Supramolecular Synthons on Surfaces: Controlling Dimensionality and Periodicity of Tetraarylporphyrin Assemblies by the Interplay of Cyano and Alkoxy Substituents**

Nikolai Wintjes,*[a] Jens Hornung,*[b] Jorge Lobo-Checa,[a] Tobias Voigt,[b] Tomás Samuely,[a] Carlo Thilgen,[b] Meike Stöhr,[a] François Diederich,*[b] Thomas A. Jung*[c]

[a]Department of Physics
University of Basel
CH-4056 Basel (Switzerland)

[b]Laboratorium für Organische Chemie
ETH-Zürich, Hönggerberg, HCI
CH-8093 Zürich (Switzerland)

[c]Laboratory for Micro- and Nanotechnology
Paul Scherrer Institute
CH-5232 Villigen PSI (Switzerland)

1. Synthesis

General

Reagents (*Aldrich, Acros, Lancaster, Fluka*) and solvents (*Fluka, J. T. Baker*) were used without further purification. 4-(3-Methylbutoxy)benzaldehyde (***12***) and 3,5-dihydroxybenzaldehyde (***5***) are commercially available. Propyl-3,4,5-tris(tetradecyloxy)benzoate (***8***)[1] and 4-(di-1*H*-pyrrol-2-ylmethyl)benzonitrile (***11***)[2] were synthesized according to the literature.

Column chromatography was performed using SiO_2-F60 (0.040-0.063 mm, 60 Å, Silicycle). Flash chromatography was performed on a Büchi Gradient Flash System using MPLC PP cartridges and SiO_2-F60 (0.040-0.063 mm, 60 Å, Silicycle). Melting points were measured on a *Büchi B-540* melting-point apparatus in open capillaries and are uncorrected.

Infrared spectra (IR) were recorded on a *Perkin-Elmer* FT1600 spectrometer. The spectra were measured in the neat state. Selected absorption bands are reported in wavenumbers (cm^{-1}) and their relative intensities are described as *s* (strong), *m* (medium) and *w* (weak).

^1H NMR (300 MHz) spectra were measured on a *Varian Gemini 300* spectrometer and are reported as follows: chemical shift δ in ppm (multiplicity, coupling constant *J* in Hz, number of protons). The residual solvent peak was used as an internal reference ($CDCl_3$: δ_H = 7.26 ppm). ^{13}C NMR (75 MHz) spectra were recorded on a *Varian Gemini 300* using signals of $CDCl_3$ (δ_C = 77.0 ppm) as a reference. All spectra were recorded at 20 °C.

Mass spectrometry was performed by the MS service at ETH Zürich. Electron impact mass spectra were measured at 70 eV on a *Hitachi-Perkin-Elmer VG-Tribrid* spectrometer. High-resolution matrix-assisted laser desorption/ionization mass spectra were measured on an *Ionspec Ultima FT-ICR* mass spectrometer using 3-hydroxypyridine-2-carboxylic acid (3-HPA) as matrix.

Experimental Protocols (Scheme SI1)

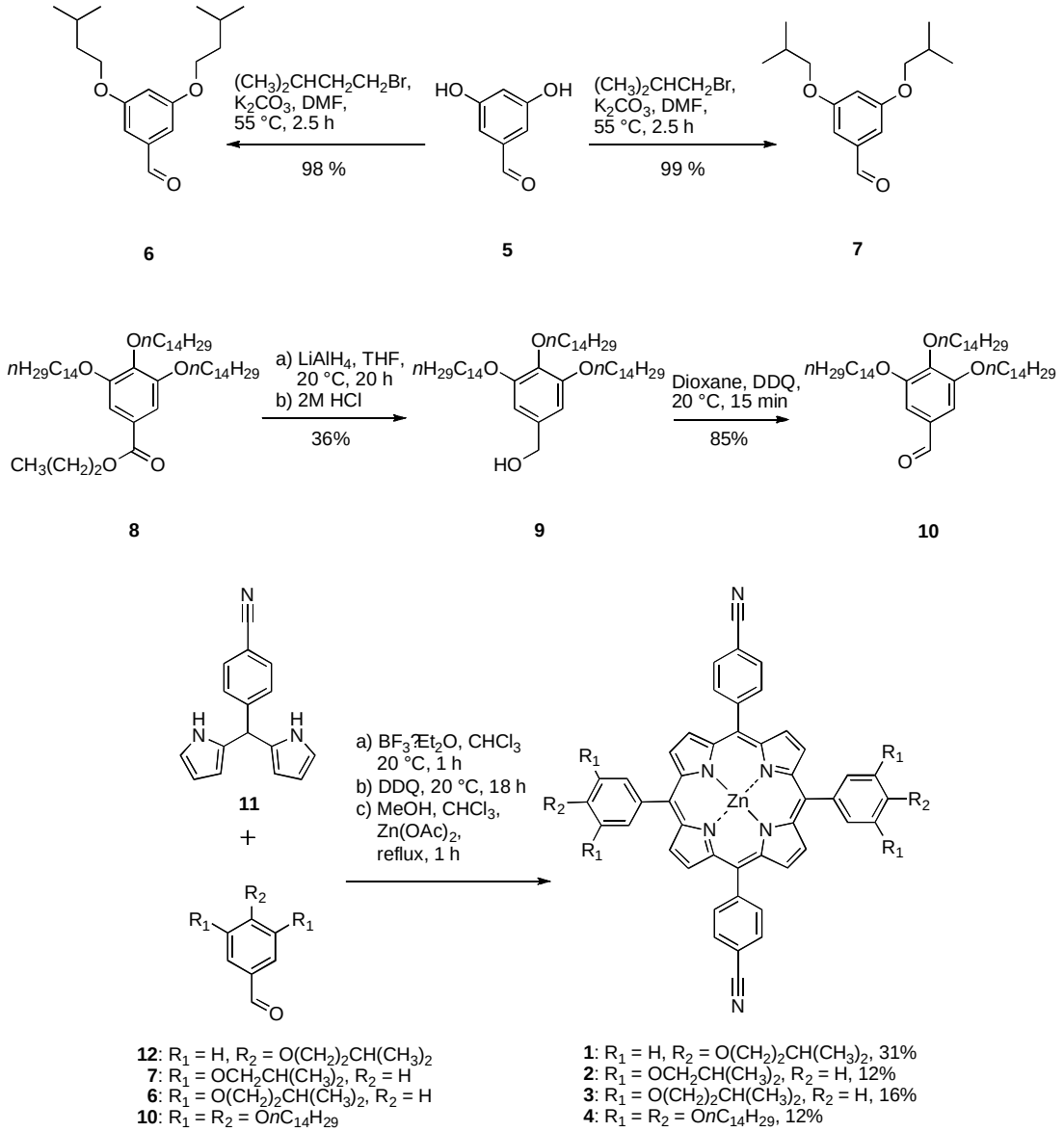

Scheme SI1: Synthesis of porphyrins **1-4**

3,5-Bis(3-methylbutoxy)benzaldehyde (*6*):

3,5-Dihydroxybenzaldehyde (***5***) (0.980 g, 7.10 mmol), K_2CO_3 (3.24 g, 23.4 mmol) and 1-bromo-3-methylbutane (4.87 g, 32.3 mmol) were dissolved in DMF (*N*,*N*-dimethylformamide, 10 mL) and stirred for 2.5 h at 55 °C. The solution was cooled to 20 °C, and water (15 mL) was added. The aqueous solution was extracted with EtOAc (3×30 mL). The combined organic phases were dried over Mg_2SO_4, concentrated *in vacuo*, and purified by flash chromatography on silica using CH_2Cl_2 as eluent, affording 1.97 g (99 %) product as a pale orange oil.

^{1}H NMR (300 MHz, $CDCl_3$): 0.97 (d, J = 6.6, 12H), 1.75-1.61 (m, 4H), 1.91-1.76 (m, 2H),

4.01 (t, *J* = 6.6, 4H), 6.70 (t, *J* = 2.3, 1H), 6.99 (d, *J* = 2.3, 2H), 9.88 (s, 1H);

^{13}C NMR (75 MHz, $CDCl_3$): 22.45, 24.94, 37.72, 66.71, 107.46, 107.89, 138.18, 160.63, 192.03;

IR (neat): 2956 (w), 2871 (w), 1689 (m), 1591 (s), 1451 (w), 1382 (m), 1295 (m), 1163 (s), 1061 (m), 844 (w), 714 (w), 676 (w);

HR-EI-MS: calculated for $C_{17}H_{26}O_3^+$: 278.1882; found: 278.1880 $[M]^+$.

3,5-Diisobutoxybenzaldehyde (*7*):

3,5-Dihydroxybenzaldehyde (***5***) (931 mg, 6.74 mmol), K_2CO_3 (3.07 g, 22.2 mmol) and 1-bromo-2-methylpropane (4.20 g, 3.64 mmol) were dissolved in DMF (10 mL) and stirred for 2.5 h at 55 °C. The solution was cooled to 20 °C, and water (15 mL) was added. The aqueous solution was extracted with EtOAc (3×30 mL). The organic phases were dried over Mg_2SO_4 and concentrated *in vacuo.* The residue was purified by flash chromatography on silica (eluent: heptane/CH_2Cl_2 100:0 → 70:30 in 50 min, flow rate 50 ml/min). The product was obtained as a clear oil. Yield: 1.68 g (99 %).

^{1}H NMR (300 MHz, $CDCl_3$): 1.02 (d, *J* = 6.6, 12H), 2.19-2.00 (m, 2H), 3.74 (d, *J* = 6.6, 4H), 6.70 (t, *J* = 2.3, 1H), 6.97 (d, *J* = 2.3, 2H), 9.87 (s, 1H);

^{13}C NMR (75 MHz, $CDCl_3$): 19.29, 28.28, 74.71, 107.45, 107.90, 138.12, 160.64, 191.79;

IR (neat): 2959 (m), 2875 (w), 1706(s), 1592 (m), 1456 (w), 1316 (s), 11.67 (m), 1048 (s), 945(m), 834 (m), 730 (m);

HR-EI-MS: calculated for $C_{15}H_{22}O_3^+$: 250.1569; found: 250.1565 $[M]^+$.

[3,4,5-Tris(tetradecyloxy)phenyl]methanol (9):

Propyl 3,4,5-tris(tetradecyloxy)benzoate **8** (5.61 g, 7.01 mmol) was dissolved in THF (tetrahydrofuran, 30 mL) and was added dropwise at 10 °C to a suspension of $LiAlH_4$ (202 mg, 5.33 mmol) in THF (30 mL). The mixture was stirred for 20 h at 20 °C, then cooled to 10 °C, and aqueous HCl (21 mL, 2 M) was added dropwise. The solution was stirred for 1 h, ice (30 g) and EtOAc (ethyl acetate, 50 mL) were added, the phases separated, and the aqueous phase was extracted with EtOAc (3 × 70 mL). The combined organic layers were

washed with saturated sodium bicarbonate ($NaHCO_3$, 70 mL), water (70 mL) and saturated aqueous NaCl solution (70 mL), dried over $MgSO_4$ and concentrated *in vacuo*. The residue was purified by flash chromatography on silica (eluent: heptane/CH_2Cl_2 100:0 → 0:100 in 100 min, flow rate 50 ml/min, UV detection at 254 nm). The product was obtained as a white solid. Yield: 1.86 g (36 %).

M.p.: 56-58 °C;

^{1}H NMR (300 MHz, $CDCl_3$): 0.95-0.82 (m, 9H), 1.53-1.20 (m, 66H), 1.89-1.68 (m, 6H), 2.28 (br s, 1H), 3.93 (t, J = 6.4, 6H), 4.54 (s, 2H), 6.51 (s, 2H);

^{13}C NMR (75 MHz, $CDCl_3$): 14.02, 22.62, 26.06, 29.32, 29.37, 29.61, 29.66,29.69, 30.24, 31.86, 65.62, 68.89, 73.32, 105.02, 136.19, 137.16, 152.98, 153.03, some signals are not visible due to overlapping;

IR (neat): 2951 (w), 2916 (m), 2849 (w), 1588 (w), 1438 (w), 1243 s), 1120 (w), 824 (s), 733 (w), 690 (m), 623 (w);

HR-EI-MS: calculated for $C_{49}H_{92}O_4^+$: 744.6996; found: 744.6975 $[M]^+$.

3,4,5-Tris(tetradecyloxy)benzaldehyde (10):

3,4,5-Tris(tetradecyloxy)phenyl)methanol **9** (950 mg, 1.28 mmol) was dissolved in dioxane (20 mL), and DDQ (2,3-dichloro-5,6-dicyano-*p*-benzoquinone, 289 mg, 1.28 mmol) was added. After 15 min, a precipitate formed and the color changed from dark green to green/yellow. The solvent was evaporated while the solution turned purple. The residue was dissolved in CH_2Cl_2 (70 ml) and filtrated. The solution was concentrated *in vacuo*. The residue was purified by flash chromatography on silica (eluent: heptane/CH_2Cl_2 100:0 → 60:40 in 35 min, flow rate 50 mL/min, UV detection at 254 nm). The product was obtained as a white solid. Yield: 807 mg (85 %).

M.p.: 62-63 °C;

^{1}H NMR (300 MHz, $CDCl_3$): 0.92-0.82 (m, 9H), 1.40-1.19 (m, 60H), 1.56-1.42 (m, 6H), 1.89-1.69 (m, 6H), 4.13-3.92 (m, 6H), 7.08 (s, 2H), 9.82 (s, 1H);

^{13}C NMR (75 MHz, $CDCl_3$): 14.23, 22.79, 26.12, 26.15, 29.33, 29.46, 29.63, 29.71, 29.79, 30.42, 32.01, 69.20, 73.60, 107.72, 131.29, 143.65, 153.33, 191.01 some signals are not visible due to overlapping;

IR (neat): 2913 (s), 2847 (s), 1691 (m), 1577 (w), 1500 (s), 1468 (m), 1440 (m), 1380 (w), 1225 (w), 1144 (m), 1118 (s), 986 (w), 966 (w), 823 (w), 719 (m), 646 (w), 615 (w);

HR-EI-MS: calculated for $C_{49}H_{90}O_4^+$: 742.6839; found: 742.6816 $[M]^+$.

General procedure for porphyrin synthesis:

GP: The aldehyde (1 eq.) and 4-(di-1*H*-pyrrol-2-ylmethyl)benzonitrile (1 eq.) were dissolved in $CHCl_3$ (70 mL/mmol aldehyde) and degassed with nitrogen for 2 h. Subsequently, $BF_3{\cdot}OEt_2$ (0.45 eq.) was added, and the mixture stirred in the dark at 20 °C for 1 h. After addition of DDQ (3 eq.), the solution was stirred for an additional 18 h. The crude mixture was filtered through a plug of silica, concentrated *in vacuo*, and dissolved in $CHCl_3$ (70 mL/mmol aldehyde). A solution of $Zn(OAc)_2$ (10 eq.) in methanol (5 mL/mmol $Zn(OAc)_2$) was added and the mixture heated to reflux for 1 h. After concentration *in vacuo*, the residue was dissolved in CH_2Cl_2 (100 mL/mmol aldehyde), washed with water, dried over $MgSO_4$, concentrated *in vacuo* and purified by flash chromatography on silica.

{5,15-Bis(4-cyanophenyl)-10,20-bis[4-(3-methylbutoxy)phenyl]porphyrinato(2–)-
k*N*^{21},k*N*^{22},k*N*^{23},k*N*^{24}}zinc(II) (*1*):

Porphyrin **1** was synthesized by **GP** using **12** (77 mg, 0.404 mmol), **11** (100 mg, 0.404 mmol), $BF_3{\cdot}OEt_2$ (22 µL, 0.18 mmol), and DDQ (275 mg, 1.21 mmol). Purification by column chromatography (eluent: CH_2Cl_2) afforded **1** (56 mg, 31 %) as a purple solid.

M.p.: decomposition > 350 °C;

^{1}H NMR (300 MHz, $CDCl_3$): 1.11 (d, *J* = 6.5, 12H), 1.86-1.94 (m, 4H), 1.93-2.15 (m, 2H) 4.30 (t, *J* = 6.5, 4H), 7.33-7.27 (m, 4H), 8.16-8.02 (m, 8H), 8.40-8.28 (m, 4H), 8.84 (d, *J* = 4.7, 4H), 9.04 (d, *J* = 4.7, 4H);

^{13}C NMR (75 MHz, $CDCl_3$): 22.66, 25.13, 38.12, 66.62, 111.54, 112.64, 118.63, 118.99, 121.71, 130.29, 131.17, 132.75, 134.35, 134.76, 135.33, 147.71, 149.17, 150.79, 158.88;

IR (neat): 2954 (w), 2921 (w), 2851 (w), 2230 (w), 1602 (m) 1494 (w), 1245 (m), 1174 (s), 995 (s), 807 (m), 793 (s), 714 (m);

HR-MALDI-MS (3-HPA): calculated for $C_{56}H_{47}N_6O_2Zn^+$: 899.3052; found: 899.3006

$[M+H]^+$.

{5,15-Bis(4-cyanophenyl)-10,20-bis[3,5-di(isobutoxy)phenyl]porphyrinato(2–)-kN^{21},kN^{22},kN^{23},kN^{24}}zinc(II) (*2*):

Porphyrin **2** was synthesized by **GP** using **7** (140 mg, 0.540 mmol), **11** (133 mg, 0.540 mmol), $BF_3{\cdot}OEt_2$ (30 µL, 0.24 mmol), and DDQ (367 mg, 1.62 mmol). Purification by flash chromatography on silica (eluent: heptane/CH_2Cl_2 100:0 → 30:70 in 50 min, 50 mL/min) afforded **2** (33 mg, 12 %) as a purple solid.

M.p.: decomposition > 350 °C;

^{1}H NMR (300 MHz, $CDCl_3$): 1.05 (d, *J* = 6.7, 24H), 2.26-2.03 (m, 4H), 3.84 (d, *J* = 6.3, 8H), 6.80-6.86 (m, 2H), 7.33 (d, *J* = 1.4, 4H), 8.06 (d, *J* = 8.0, 4H), 8.34 (d, *J* = 8.0, 4H), 8.84 (d, *J* = 4.7, 4H), 9.12 (d, *J* = 4.7, 4H);

^{13}C NMR (75 MHz, $CDCl_3$): 19.43, 28.45, 74.76, 101.03, 111.57, 114.35, 118.66, 1118.96, 121.73, 130.28, 131.18, 132.77, 134.69, 143.82, 147.65, 149.26, 150.11, 158.13;

IR (neat): 2956 (w), 2870 (w), 2227 (w), 1589 (s), 1433 (m), 1352 (m), 1154 (s), 1060 (m), 1031 (m), 997 (s), 796 (s), 776 (m), 718 (m);

HR-MALDI-MS (3-HPA): calculated for $C_{62}H_{58}N_6O_4Zn^+$: 1014.3811; found: 1014.3824 $[M]^+$.

{5,15-Bis[3,5-bis(3-methylbutoxy)phenyl]-10,20-bis(4-cyanophenyl)porphyrinato(2–)-kN^{21},kN^{22},kN^{23},kN^{24}}zinc(II) (*3*):

Porphyrin **3** was synthesized by **GP** using **6** (112 mg, 0.404 mmol), **11** (100 mg, 0.404 mmol), $BF_3{\cdot}OEt_2$ (22 µL, 0.18 mmol), and DDQ (275 mg, 1.21 mmol). Purification by column chromatography on 120 g of silica (eluent: CH_2Cl_2) afforded **3** (35 mg, 16 %) as a purple solid.

M.p.: decomposition > 350°C;

^{1}H NMR (300 MHz, $CDCl_3$): 0.97 (d, J = 14.9, 24H), 1.80-1.70 (m, 8H), 1.95-1.80 (m, 4H), 4.14 (t, *J* = 6.7, 8H), 6.89 (t, *J* = 2.3, 2H), 7.36 (d, *J* = 2.3, 4H), 8.07 (d, *J* = 8.4, 4H), 8.34 (d, *J* = 8.4, 4H), 8.82 (d, *J* = 4.7, 4H), 9.11 (d, *J* = 4.7, 4H);

^{13}C NMR (75 MHz, $CDCl_3$): 22.73, 25.19, 38.10, 66.77, 100.94, 111.58, 114.38, 118.67, 118.96, 121.66, 130.28, 131.18, 132.76, 134.70, 143.84, 147.63, 149.26, 150.09, 157.96;

IR (neat): 2954 (w), 2922 (m), 2854 (w), 2228 (w), 1600 (m), 1585 (s), 1430 (m), 1352 (m), 1159 (s), 1052 (s), 997 (s), 809 (m), 798 (s), 718 (m);

HR-MALDI-MS (3-HPA): calculated for $C_{66}H_{66}N_6O_4Zn^+$: 1070.4437; found: 1070.4411 $[M]^+$.

{5,15-Bis(4-cyanophenyl)-10,20-bis[3,4,5-tris(tetradecyl)phenyl]porphyrinato(2–)-kN^{21},kN^{22},kN^{23},kN^{24}}zinc(II) (*4*):

Porphyrin **4** was synthesized by **GP** using **10** (392 mg, 0.527 mmol), **11** (130 mg, 0.527 mmol), $BF_3{\cdot}OEt_2$ (29.1 µL, 0.237 mmol) and DDQ (358 mg, 1.58 mmol). Purification by flash chromatography on silica (eluent: heptane/CH_2Cl_2 100:0 → 30:70 in 50 min, 50 mL/min) afforded **4** (62 mg, 12 %) as a purple solid.

M.p.: 205-209 °C;

^{1}H NMR (300 MHz, $CDCl_3$): 1.01-0.79 (m, 18H), 1.59-1.12 (m, 128H), 1.76-1.61 (m, 4H), 1.92-1.80 (m, 8H), 2.06-1.92 (m, 4H), 4.07 (t, *J* = 6.1, 8H), 4.28 (t, *J* = 6.3, 4H), 7.42 (s, 4H), 8.08 (d, *J* = 7.5, 4H), 8.38 (d, *J* = 8.1, 4H), 8.87 (d, *J* = 4.7, 4H), 9.14 (d, *J* = 4.7, 4H);

^{13}C NMR (75 MHz, $CDCl_3$): 14.04, 22.60, 22.65, 22.65, 26.07, 26.26, 29.27, 29.38, 29.56, 29.61, 29.66, 29.70, 29.75, 29.78, 29.97, 30.54, 31.83, 31.90, 69.29, 73.65, 111.66, 114.31, 118.75, 118.93, 122.00, 130.34, 131.27, 132.83, 134.73, 137.12, 137.92, 147.66, 149.34, 150.49, 151.03, some signals are not discernible due to overlap;

IR (neat): 2920 (s), 2851 (s), 2228 (w), 1578 (w), 1467 (w), 1418 (w), 1380 (w), 1345 (m), 1328 (m), 1112 (s), 1073 (w), 998 (m), 807 (m), 721 (w);

HR-MALDI-MS (3-HPA): calculated for $C_{130}H_{195}N_6O_6Zn^+$: 2000.4424; found: 2000.4469 $[M+H]^+$.

2. High-vacuum Sublimation Apparatus

For the high-vacuum sublimation apparatus (Figure SI1), the following devices were purchased from Ilmvac GmbH, D-98693 Ilmenau, Germany:

KF 40 flanges made of borosilicate glass 3.3 or quartz glass, KF 40 centering rings for glass-glass-flanges, and glass-metal-flanges with aluminium connections and Viton compound O-ring, KF 40 clamping chains synthetic.

For heating, a hot plate “SH 85” from Gestigkeit GmbH, D-40489 Düsseldorf, Germany and a tin bath were used. Wood’s metal is not suitable, since the cadmium shows a noticeable vapour pressure at the sublimation temperatures (1 mbar at 380 °C, 10 mbar at 470 °C).

The bigger part of the high vacuum sublimation apparatus (including a cold finger, cold trap and flanges for connection to the turbomolecular pump) is made of borosilicate glass 3.3, the flask which dips into the tin bath is made of quartz glass.

In a typical sublimation experiment, 1-2 mg of the porphyrin were placed into the quartz flask, the apparatus was closed and evacuated using a turbomolecular pump at = 10^{-5} mbar (oil diffusion pump could be used as well). The cold trap was filled with liquid nitrogen, the tin bath heated to 232 °C (melting point of tin), the quartz flask was immersed, and the bath further heated at a rate of 20 °C/min. When the porphyrin started to sublime, the heating rate was lowered to 5 °C/min until all of the product sublimed or it was stopped at a temperature of 480 °C.

After cooling, the sublimed product (and, if necessary, the residue in the quartz tube) was washed off the cold finger with 1 mL of $CDCl_3$. The product was analyzed by means of ^{1}H NMR and MALDI-MS.

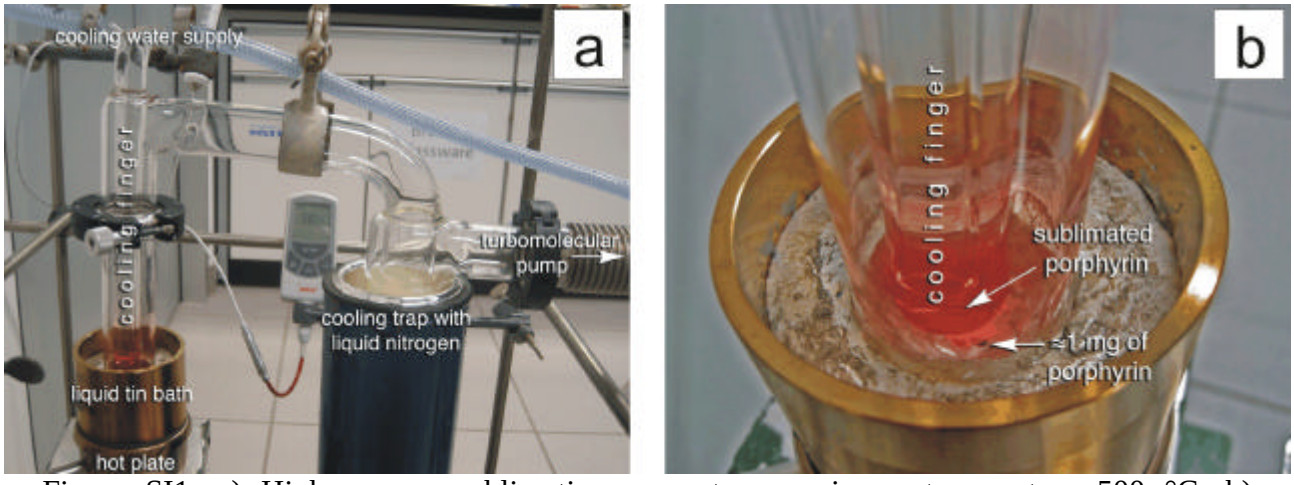

Figure SI1. a) High-vacuum sublimation apparatus, maximum temperature 500 °C. b) Detailed view of the tin bath and the cold finger with the sublimed porphyrin.

Porphyrins **1**-**3** were sublimed at a tin bath temperature of 380°C. The structural integrity of the sublimed material was verified by ^{1}H NMR and MALDI-MS.

Porphyrin **4** was sublimed at a temperature of 420°C. MALDI analysis of the red deposit at the cold finger showed that most of the product had decomposed during the sublimation process. According to the MALDI spectrum, one or more tetradecyl chains were cleaved off the aryl substituent (Figure SI2) Furthermore, the porphyrin did not evaporate completely, leaving an insoluble black residue in the sublimation flask.

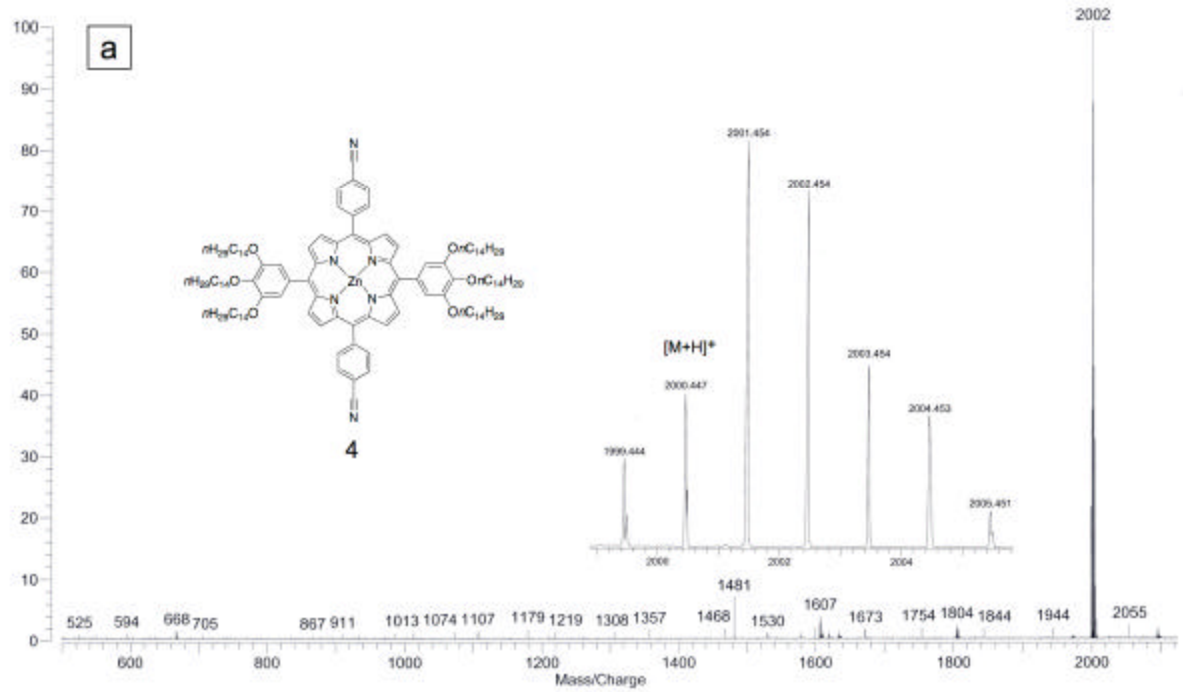

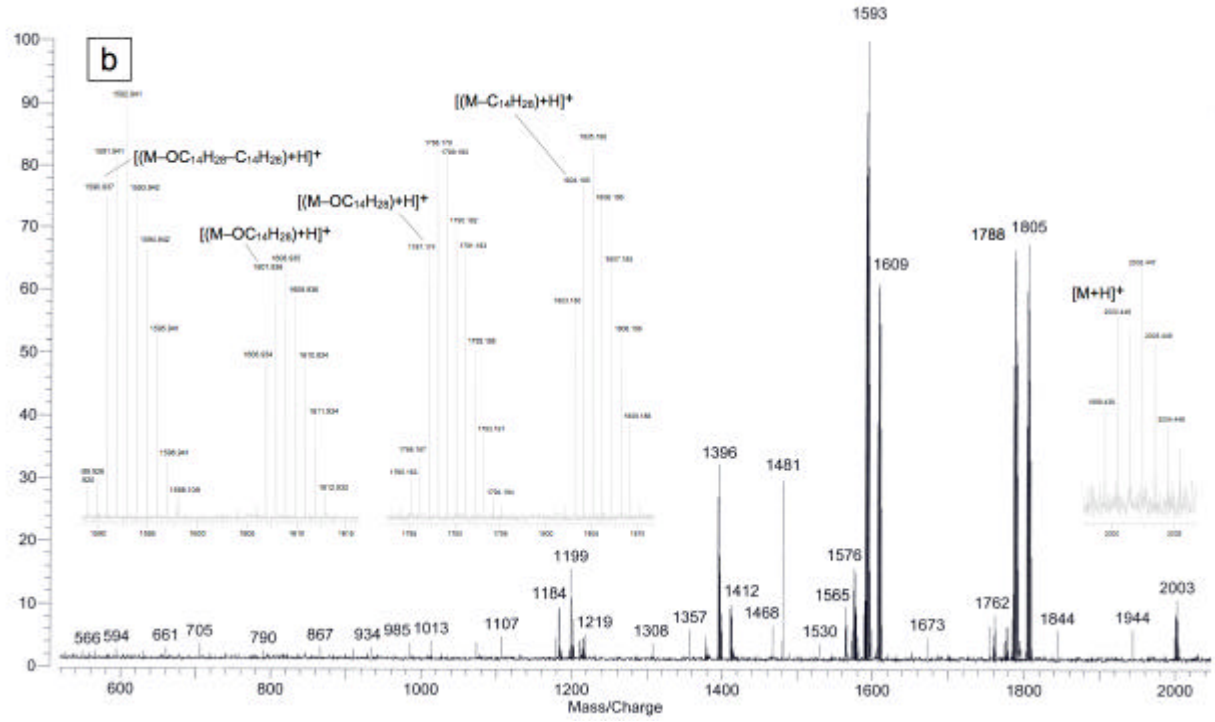

Figure SI2. a) MALDI-MS of porphyrin **4.** b) MALDI-MS of the sublimation product of porphyrin **4**. The fragmentation pattern indicates breaking of C–O bonds.

3. Controlled Switching between Imaging Modes

As stated in the main text, two characteristically different imaging modes were used, in which either the p-system gives a strong signal (p-imaging mode, 1 in Figure SI3), or all parts of the molecule are equally visible (full imaging mode, 2 in Figure SI3). The mode of imaging does not change with the applied voltage. However, by applying small voltage pulses of ca. 3.5 V, one can sometimes switch between the modes in a random way, as shown in Figure SI3. Occasionally, a third mode (mode 3) was seen, in which the alkoxy chains are accentuated, as well as a mixed mode (2 / 3). We think that the different imaging modes can be attributed to different tip conditions: Probably, the tip apex is changed due to the picking up or the release of organic particles.

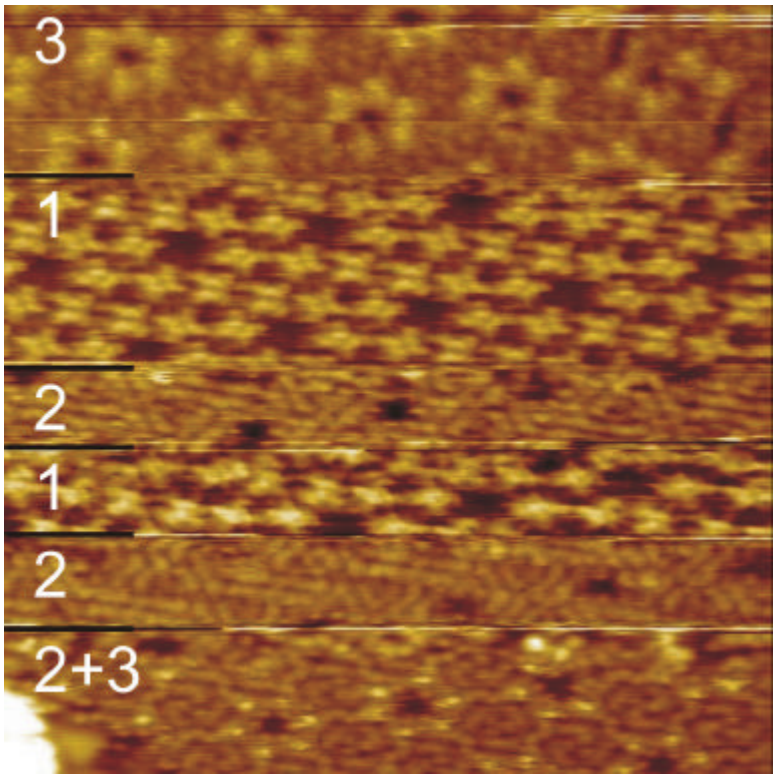

Figure SI3. STM image of molecule **2** on Cu(111) at a coverage > 0.8 ML (ML = monolayer) (25 × 25 nm^2; U = -1.4 V, I = 20 pA). The image shows that switching between the characteristic imaging modes (1: p-imaging mode, 2: all parts of the molecules give equal contrast, 3: the mobile alkoxy chains give the dominant signal) can be achieved by applying voltage pulses.

4. Alignment of the Molecules within the Chains with Respect to the Copper Substrate

Figure SI4a shows an STM image of chains of molecule **3** on a Cu(111) surface. Both atomic resolution of the substrate and molecular resolution of the chains were obtained simultaneously. Interestingly, not all parts of the bare metal substrate are atomically resolved. This effect can be related to an individual molecule, which is trapped at the apex of the scanning tip and dragged over the substrate before it is stripped off at the next molecular chain.[3]

From such an image, we were able to determine the orientation of the molecules with respect to the substrate. We emphasized for each molecule the position of its characteristic dark line which bisects each porphyrin core and originates from two downward-tilted pyrrole rings (see main text; black lines in Figure SI4a). In total, three different directions were found, two of them always including an angle of approximately 120 degrees.

The derivative of the STM image clearly shows the principal directions of the Cu(111) substrate (Figure SI4b, green star). By superposition of the topographic STM image (Figure SI4a) and its derivative (Figure SI4b), the three molecular orientations can be related to the principal directions of the substrate (green and black star in Figure SI4c). It has to be kept in mind that, in STM images, drift effects are reflected much more strongly in the slow scanning direction (here the vertical direction) than in the fast one (horizontal direction). Furthermore, the principal directions of the substrate can be determined with a higher precision than those of the dark lines, because of the small dimensions of an individual molecule. Nevertheless, the result shows that, within an uncertainty of 5 degrees, the characteristic dark lines follow the principal directions of the substrate.

The angle between the dark line, representing a diagonal through the porphyrin core, and the direction along the cyanophenyl groups amounts to 135 degrees (anticlockwise). As the angle between the principal directions of the substrate is 120 degrees, straight sections within the molecular chains are tilted by an angle of (15 ± 5) degrees against the principal directions.

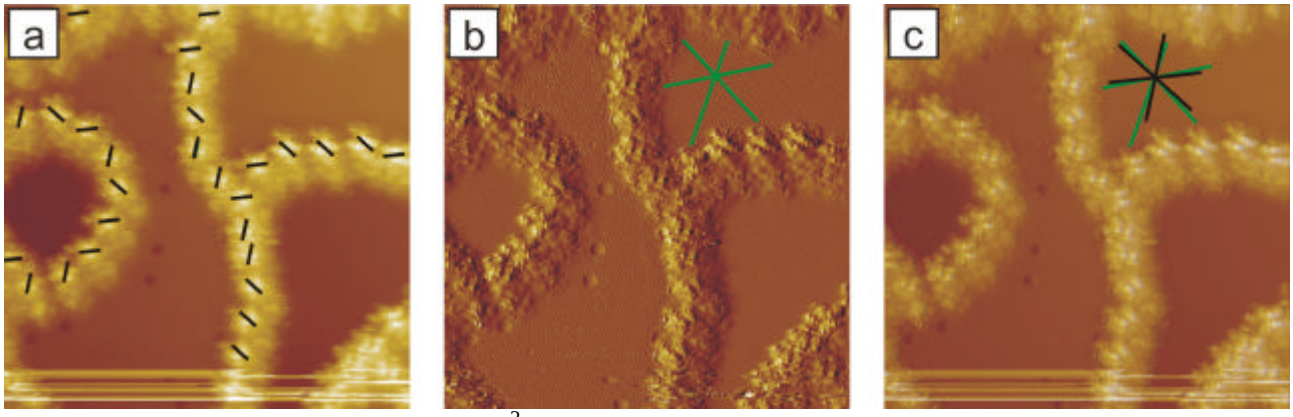

Figure SI4. a) STM image (25×25 nm^2; U = +0.9 V, I = 10 pA) of molecule **2** on Cu(111) at a coverage of about 0.2 ML. Both atomic resolution of the substrate and molecular resolution of the chains is achieved. The black lines emphasize the direction of the characteristic dark line in each molecule. b) In the derivative of the STM image, the atomic resolution is more accentuated and thus, the three principal directions pf the substrate (indicated by the green star) can be easily identified. c) By overlaying the STM image with its derivative we can directly compare the directions of the characteristic dark line (black star) with the atomic directions (green star).

5. Density-dependent Images of the Molecular Chains Hinting at the Formation of the Networks

Figure SI5 shows STM images of the molecular chains with the coverage increasing from image (a) to (d). At low coverage, the chains show nearly no branching, whereas with increasing coverage, the number of branches grows. At very high coverages (about 0.8 ML, Figure SI5d), the formation of single pores can be observed (white circles in Figure SI5d). Hence, the transition from the chainlike arrangements of **2** and **3** to the respective networks is caused by the decreasing space available for the molecules and the growth of the networks starts with a single pore.

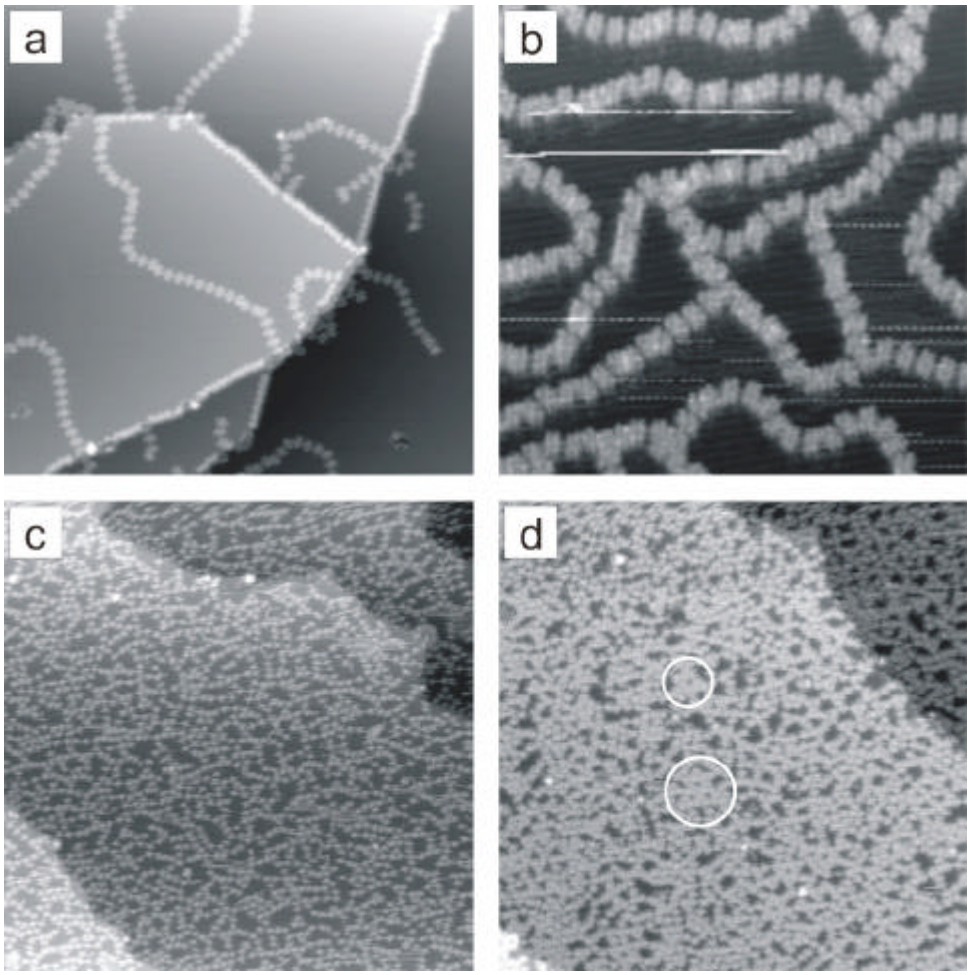

Figure SI5. STM images of the molecular chains with increasing coverages. a) (100 × 100 nm^2; U = -1.5 V, I = 20 pA) Approx. 0.1 ML. No branching is observed. b) (50 × 50 nm^2; U = -1.4 V, I = 10 pA) Approx. 0.3 ML and c) (100 × 100 nm^2; U = -1.5 V, I = 20 pA) Approx. 0.7 ML. The number of branches grows with increasing coverage. d) (100 × 100 nm^2; U = -1.5 V, I = 20 pA) Approx. 0.8 ML. Single pores, marked by white circles, are formed.

6. References

[1] H. Adams, C. A. Hunter, K. R. Lawson, J. Perkins, S. E. Spey, C. J. Urch, J. M. Sanderson, *Chem. Eur. J.* **2001**, *7*, 4863.

[2] P. D. Rao, S. Dhanalekshmi, B. J. Littler, J. S. Lindsey, *J. Org. Chem.* **2000**, *65*, 7323.

[3] M. Böhringer, W.-D. Schneider, R. Berndt, K. Glockler, M. Sokolowski, E. Umbach, *Phys. Rev. B* **1998**, *57*, 4081.